Journal of Materials Chemistry A

PAPER

View Article Online
View Journal | View Issue

Cite this: J. Mater. Chem. A, 2014, 2, 365

Ion conduction and phase morphology in sulfonate copolymer ionomers based on ionic liquid–sodium cation mixtures†

Siti Aminah Mohd Noor,[ab] Daniel Gunzelmann,[d] Jiazeng Sun,[a] Douglas R. MacFarlane[ac] and Maria Forsyth*[cd]

Received 24th September 2013
Accepted 7th November 2013

DOI: 10.1039/c3ta13835f

www.rsc.org/MaterialsA

A series of sulfonate based copolymer ionomers based on a combination of ionic liquid and sodium cations have been prepared in different ratios. This system was designed to improve the ionic conductivity of ionomers by partially replacing sodium cations with bulky cations that are less associated with anion centres on the polymer backbone. This provides more conduction sites for sodium to 'hop' to in the ionomers. Characterization showed the glass transition and ^{15}N chemical shift of the ionomers did not vary significantly as the amount of Na^+ varied, while the ionic conductivity increased with decreasing Na^+ content, indicating conductivity is increasingly decoupled from T_g. Optical microscope images showed phase separation in all compositions, which indicated the samples were inhomogeneous. The introduction of low molecular weight plasticizer (PEG) reduced the T_g and increased the ionic conductivity significantly. The inclusion of PEG also led to a more homogeneous material.

Introduction

Polymer electrolytes are of immense interest due to their applicability in energy conversion and storage devices such as fuel cells and batteries. They present significant advantages over liquid electrolytes and ceramic electrolytes, on one hand due to the removal of volatile, liquid components and on the other hand their potential flexibility and moldability. Polymer electrolytes have been under investigation since the late 1970s when Wright *et al.*[1] discovered that polyether complexes of alkali salts were ionically conductive and later Armand *et al.*[2,3] suggested these could potentially be useful in solid state batteries.

Over the past three decades there has been intense research in trying to improve the ionic conductivity in solid polymer electrolytes.[4] Amorphous polyethylene oxide (PEO) based systems have generally shown the highest conductivity, with some significant improvement in properties and conductivity obtained by using nanofillers in PEO based solid polymer electrolytes (SPEs).[5–9] One desirable property in any given electrolyte is a high transport number for the target ion of interest; for example lithium ion for a lithium battery, protons in the case of proton membrane fuel cells and sodium if we consider a sodium device. In devices utilizing a cation charge carrier, anion mobility is undesirable, as the device would then suffer from undesirable concentration polarization, in which anion build up occurs at the electrode/electrolyte interface due to its high mobility in the electrolyte, and this concentration polarization diminishes battery performance.[10]

One method of achieving only cation conductivity in a polymer system is to tether the anion to the polymer backbone, as in a polyelectrolyte or an ionomer system. Numerous single-ion conductor ionomer systems have been developed over the years; for example those based on poly(2-acrylamido-2-methyl-1-propane-sulfonic acid) (PAMPS)[11,12] and copolymers of sulfonate polyester, sulfonated ethylene/styrene and styrene-ethylene/butylene-styrene.[13–17] In general, however, the anion on the polymer backbone is somewhat basic, from which the cation does not readily dissociate, resulting in low ionic conductivity. A number of methods have been employed in an attempt to increase the ionic conductivity; for example the AMPS monomer has been copolymerized with *N*,*N*′-dimethylacrylamide (DMAA) to separate the ionic moieties along the backbone and thereby avoid multiple anion association to the cation.[18] The addition of an organic solvent or ionic liquid has been shown to assist lithium ion dissociation from the backbone leading to high ionic conductivities and good performance in Li-ion batteries.[11,19–22] Whilst these materials retain good elastomeric, solid-state properties, they nevertheless still contain a low molecular weight solvent that could either leak or

[a]School of Chemistry, Monash University, Clayton Campus, Victoria, Australia
[b]Chemistry Department, Centre for Defence Foundation Studies, National Defence University of Malaysia, 57000, Kuala Lumpur, Malaysia
[c]ARC Centre of Excellence for Electromaterials Science (ACES), Australia
[d]Institute for Frontier Materials Deakin University, Victoria, Australia. E-mail: maria.forsyth@deakin.edu.au

† Electronic supplementary information (ESI) available. See DOI: 10.1039/c3ta13835f

be volatile. Therefore it is still desirable to prepare solvent free, or very low solvent content, polymer electrolytes.

Recently, Colby *et al.* have investigated cation dynamics in polyester based ionomers and sulfonated polystyrene, with a variety of cations ranging from the inorganic Na^+, Li^+ and Cs^+, to organic cations which are typically used to prepare ionic liquid salts.[23] It was very interesting to observe that the glass transition temperatures of these ionomers were significantly reduced when the organic cations were used as the ionomer charge carriers, with the ionic conductivity increasing by as much as 10^4 times when a tetrabutylammonium ion was used instead of a sodium cation.[24] This was attributed primarily to a lowering in the glass transition temperature, T_g, due to the weaker electrostatic interactions between the cation and the backbone-tethered sulfonate anion. Interestingly, when the conductivities were scaled with T_g, it was apparent that the ionic transport was still intimately coupled to the polymer backbone mobility, just as is observed in PEO based polymer electrolytes where a lithium salt is dissolved in the polymer. Under such circumstances, the conductivity can only be improved by further reducing T_g. On the other hand, rigid ceramic materials such as lithium aluminium titanium phosphtate (LATP)[25,26] or β-alumina[27,28] have extraordinarily high single ion conduction, completely decoupled from the rigid nature of the host ceramic. It was postulated that the mechanism for such high single ion transport lies in multiple equi-energy sites available to charge carriers, such that ions can 'hop' from site to site relatively unencumbered.

Our hypothesis is that a similar mechanism can be designed to achieve high ionic conductivity in an ionomer system, by creating anion centres on the polymer that are less associated with the corresponding counterions and therefore the cation motion is less coupled to the bulk dynamics of the material. Essentially, by replacing a fraction of the sodium ions with a bulky ionic liquid cation, more anion sites become available to the sodium and therefore its diffusive motion more facile. The variable cation composition in such systems allows us to explore a spectrum of degrees of decoupling over quite a wide range from strongly coupled to significantly decoupled. Furthermore, the use of the flexible organic counterions should serve to decrease the T_g, as was shown by Colby *et al.*,[24] which could lead to still higher ionic conductivities and improved mechanical properties of the ionomer electrolytes.

In this paper, we prepare a series of ionomers by copolymerizing a sodium vinyl sulfonate (NaVS) monomer, and AMPS-triethylmethylammonium monomer in different ratios. These materials are characterized using a.c. impedance to measure ionic conductivity, optical microscopy to observe the morphology and variable temperature, multi-nuclear solid-state NMR spectroscopy to study the dynamic behaviour of the ionomers.

Materials and experimental

Sample preparation

Preparation of copolymers of 2-acrylamido-2-methyl-1-propanesulfonate (AMPS) (as the alkyl-ammonium/sodium salts) and the sodium salt of vinyl sulfonate (NaVS) was carried out based on Scheme 1. Typical procedures for synthesis were as follows: 5.017 g of AMPS (0.0241 mol, Aldrich) was dissolved in 10 ml of distilled water; NaVS was added drop-wise at room temperature with magnetic stirring; N_{1222}-carbonate solution (Aldrich) was added until the pH of the solution reached 7; ~0.2% of $K_2S_2O_8$ was then added into the solution and stirred at ~85 °C for

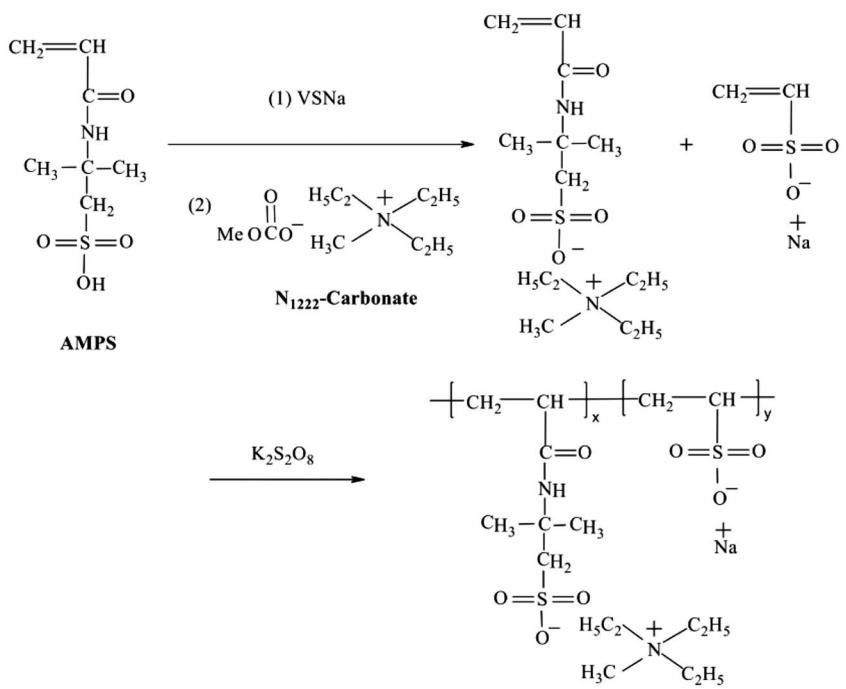

Scheme 1 Schematic preparation of poly([N_{1222}][AMPS]-*co*-Na[VS]) ionomers.

2 days. After removing the solvents from the reaction mixture the samples were dried under vacuum at ~70 °C for at least 2 days prior to any characterisation. Mole ratio of $[N_{1222}][AMPS]$ and NaVS was varied from 90 : 10 to 50 : 50.

Ionic conductivity

The ionic conductivity of the ionomers was measured by ac impedance spectroscopy using a high frequency response analyzer (HFRA; Solartron 1296). Handled in the dry box, the dried powder samples were first pressed into pellets (1 mm thick and 13 mm in diameter) using a KBr die and a hydraulic press at 10 tonne for 30 min; pellets were aged in the oven at 393 K overnight and then sandwiched between two stainless steel blocking electrodes. The sample was also further heated up to 120 °C in the conductivity barrel cell before conductivity measurement started. Data was collected over a frequency range of 0.1 Hz to 10 MHz (ten points per decade) with a 30 mV amplitude over a temperature range of 298 to 423 K in 10 K intervals. The temperature was controlled to within 1 K using a Eurotherm 2204e temperature controller and a band heater with a cavity for the cell using a thermocouple type T, which was embedded in the cell. The sample was held for a short equilibration time, up to 2 min, to stabilize the temperature prior to impedance measurement. The conductance was determined from the impedance data using the touch down of the semi-circle fit in *Z*-view (Version 2.3).

Differential scanning calorimetry (DSC)

DSC measurements were carried out on the as prepared samples, using a DSC Q100 series instrument (TA Instruments), and the data was evaluated with Universal Analysis 2000 software. Approximately 8 to 10 mg of the ionomer sample was tested over a temperature range of 273 to 423 K at a scanning rate of 10 K min^{-1}. The glass transition temperature was determined from the onset of the heat capacity change on heating ramp.

Solid-state nuclear magnetic resonance (NMR)

Solid-state NMR spectra were recorded with a BRUKER Avance III 300WB spectrometer operating at 300.13, 79.39, 75.46 and 30.42 MHz for ^{1}H, ^{23}Na, ^{13}C and ^{15}N, respectively. All ^{1}H and ^{13}C spectra are given relative to tetramethylsilane, ^{15}N spectra with respect to nitromethane and ^{23}Na spectra were referenced to 1 M $NaCl_{(aq.)}$. Samples were packed in standard 4 mm MAS rotors, loaded and measured in a 4 mm double-resonance MAS probe (BRUKER) spinning at 10 kHz. Cross-polarization from ^{1}H was used to excited ^{13}C and ^{15}N nuclei applying a ramped (50 to 100% power) shape pulse on the proton frequency with a contact time of 2–10 ms and a SPINAL64 proton decoupling with an nutation frequency of 114 kHz was applied during acquisition. Recycle delays were set between 3 and 5 times the proton T_1 relaxation constants, which were determined from earlier spectra. Static ^{1}H and ^{23}Na spectra were measured with a solid-echo sequence using a 2.5 μs 90 degree pulse and an echo delay of 20 μs.

Optical microscopy

Optical micrographs were recorded through a microscope equipped with a digital camera (Nikon D200). Images were taken directly from the surface of aged pellet samples at room temperature after conductivity measurements.

Results and discussion

Thermal properties

Fig. 1 shows the DSC thermogram of ionomers for the first scan (top) and second scan (bottom). It can be seen that there is endothermic peak (T_g overshoot) in the first thermal cycle, which is more obvious at lower concentration of Na^{+}. According to Berens and Hodge[29,30] an enthalpy overshoot at T_g is often observed in polymers when structural relaxation takes place near T_g. However, during the subsequent scans, the enthalpy overshoot no longer appeared, and only a broad T_g can be reproducibly observed. This broad T_g suggests that the sample

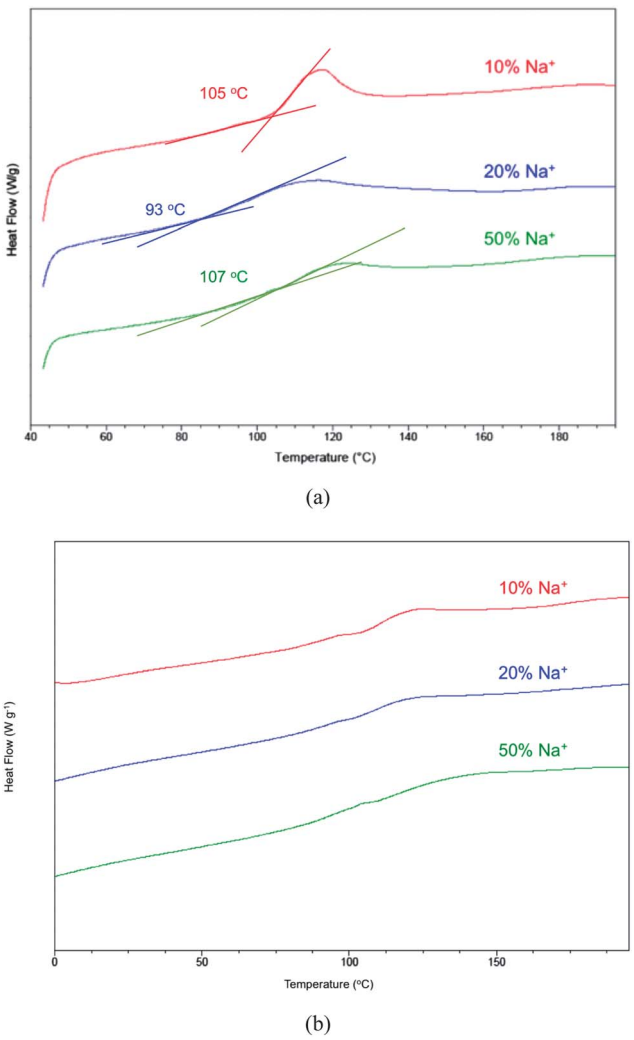

Fig. 1 DSC thermograms of poly($[N_{1222}][AMPS]$-*co*-Na[VS]) ionomers with different mol% of NaVS (a) first thermal cycle and (b) second and subsequent cycles.

is not completely homogeneous at the molecular level. This behavior will be further discussed below. Overall, these thermograms suggest that T_g does not vary significantly as the amount of sodium changes from 10–50 mol%. This is in contrast to expectations, given that Colby *et al.*[10,23,24] reported that the T_g of ionomers was reduced significantly when the ionic liquid cation was used instead of Na^+. However, in those systems, 100% of the ions were exchanged and therefore the residual Na^+ ions in the present ionomers may influence T_g significantly. The composition dependence of T_g is discussed in more detail with respect to conductivity below.

Ionic conductivity

The ionic conductivity of the ionomers was measured both during one full cycle of heating (40 °C to 150 °C) and then on subsequent cooling (150 °C to 40 °C) to observe the reproducibility and any hysteresis that might be present. Fig. 2 presents the Nyquist plots for the ionomer containing 10% Na^+ at 60, 70, 80 and 100 °C. We observed that, during the heating cycle, a second semicircle appeared in the impedance diagrams for temperatures below 100 °C. This suggests two conduction processes are present and, as with the DSC data, may reflect an inhomogeneous material in which two different transport mechanisms exist. The change in impedance of the lower frequency arc is more rapid with temperature than the high frequency arc and, above T_g, the semicircles merge leading to a single apparent conduction process. On cooling, only this single process is observed, even below T_g. Subsequent heating/cooling cycles showed reproducible behaviour with two processes always appearing at temperatures below T_g upon heating. The implications of this for the phase behaviour will be discussed further below.

Fig. 3a inset shows similar behavior for the sample containing 50% Na^+, whereby two semicircles can be observed during the heating cycle for temperatures below T_g. Fig. 3 shows the Arrhenius plot for this sample, which appears to follow Arrhenius behaviour over this temperature range above and below T_g. The blue square data points show the ionic conductivity for the second process at lower frequency. In this case, the conductivity determined from the second process at 100 °C is actually higher than the process that dominates above T_g and the higher activation energy (160 compared with 212 kJ mol^{-1}) for the low frequency process is evident in Fig. 3a. Once again, a single impedance arc is seen at all temperatures upon cooling (Fig. 3b), as was the case for the 10% Na^+ sample shown in Fig. 2.

Fig. 4 presents the Arrhenius plots for each of the ionomers with various compositions, from 0 to 100% NaVS. The 100% Na^+ ionomer shows very low conductivity, probably due to strong association of Na^+ to the sulfonate anion from the backbone, as has previously been reported for Na^+ based ionomers.[23] On the other hand, below 50% of Na^+, the ionic conductivity follows an Arrhenius behaviour, indicating a thermally activated conduction process that persists even below T_g. Indeed there is no apparent rapid decrease as T_g is approached, in contrast to the data trends observed in polyester sulfonate ionomers with ionic

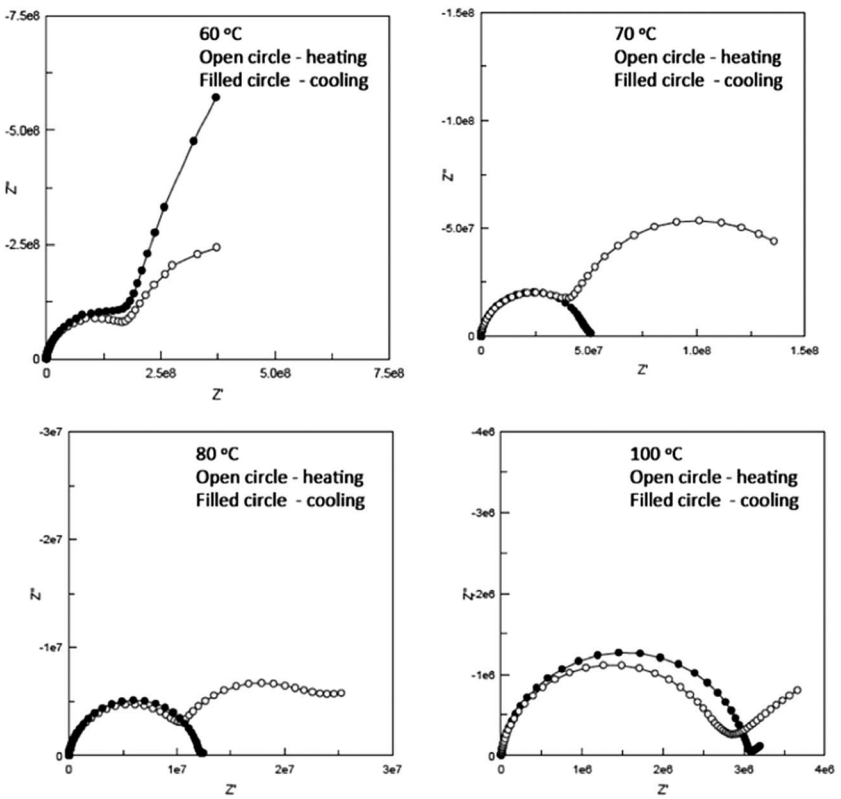

Fig. 2 Impedance plane plots of poly([N_{1222}][AMPS]-*co*-Na[VS]) ionomers with 10% NaVS.

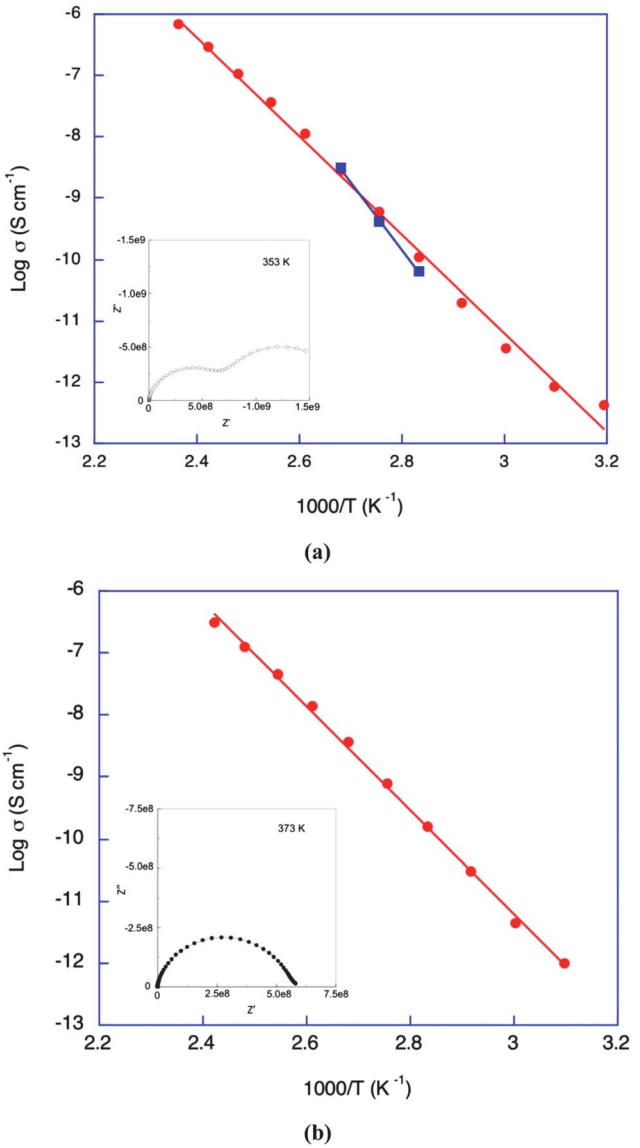

Fig. 3 Impedance plane plots and the conductivity of poly([N_{1222}][AMPS]-*co*-Na[VS]) ionomer with 50% NaVS (a) heating (b) cooling cycle. The squares are the conductivity values from the low frequency process.

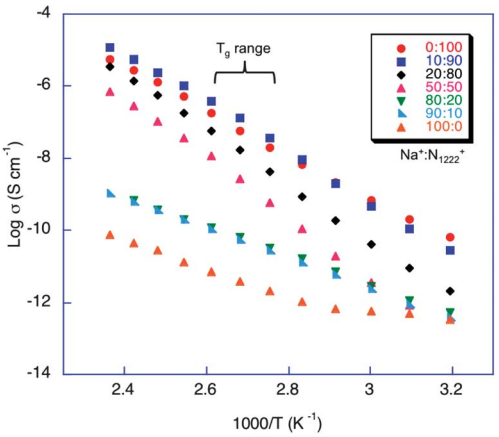

Fig. 4 Ionic conductivity of poly([N_{1222}][AMPS]-*co*-Na[VS]) ionomers with various mol% of NaVS.

Table 1 Arrhenius parameters of poly([N_{1222}][AMPS]-*co*-Na[VS]) ionomers with various mol% of NaVS

Na^+ (mol%)	E_a (kJ mol^{-1})	Log (σ_o / S cm^{-1})	r^2
0	117 ± 2	9.2 ± 0.2	0.999
10	133 ± 2	11.6 ± 0.3	0.999
20	147 ± 1	12.8 ± 0.2	0.999
50	160 ± 2	13.7 ± 0.3	0.999
80	77 ± 1	0.6 ± 0.1	0.999
90	80 ± 1	0.9 ± 0.1	0.999
100	57 ± 1	−3.3 ± 0.6	0.973

liquid counterion systems,[10,24] where conductivity approached 10^{-12} S cm^{-1} at T_g. In the work by Colby *et al.*,[24] despite the T_g decreasing as the counterion was fully replaced by an ionic liquid cation, the conductivity still remained coupled to T_g. In the present systems, the conductivity appears increasingly decoupled from the T_g of the ionomer system, particularly for compositions below 50% Na^+. An interesting, reproducible observation is that above its T_g, the 10% Na^+ sample has the highest conductivity of all the systems investigated here. Therefore it appears that mixing the two cations leads to favorable properties for conductivity in these materials. The activation energy also seems to be composition dependent, decreasing with increasing ammonium cation content as represented in Table 1.

The composition dependence of conductivity and its relationship to T_g is more clearly shown in Fig. 5, which presents the measured conductivity at 373 K together with the T_g for each of the compositions. From this data it can be seen that with addition of 10 mol% of Na^+, the ionic conductivity of the ionomer increases by a factor of two relative to the 100% poly([N_{1222}][AMPS]) sample. However, as sodium concentration is further increased, the ionic conductivity decreases dramatically, especially at 90 mol% of Na^+. The primary reason for this

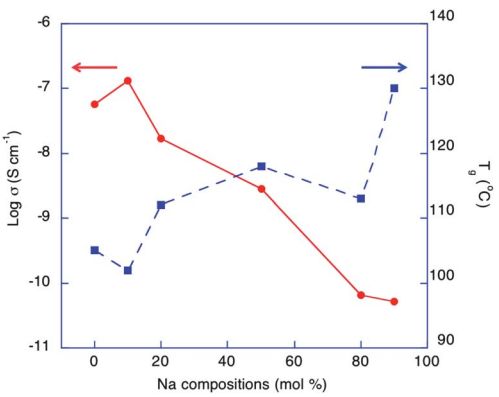

Fig. 5 Ionic conductivity at 373 K and glass transition temperature (T_g) of poly([N_{1222}][AMPS]-*co*-Na[VS]) ionomers (90 : 10) as a function of Na^+ concentration.

appears to be the increase in glass transition temperature for the ionomer with increasing Na^+ content. Even though there appears to be decoupling of conductivity from T_g, (*i.e.* there is significant measurable conductivity even below T_g) the higher the Na content the lower the extent of decoupling. In other words, as we approach 100% Na the conductivity (and hence ion mobility) at T_g is very low, indicating that the ion motion (both organic cation and Na^+) is more strongly linked to local polymer motions. The extent to which the conductivity is due to the N_{1222}^+ cation or the Na^+ cation motion cannot be determined at this stage.

Morphology

As discussed in the DSC and conductivity sections, the broad T_g that is observed and also the two semicircles seen in the Nyquist plot may be due to the sample being inhomogeneous. Fig. 6 depicts the optical microscope images for ionomers with different compositions of Na^+. Here we can clearly see that phase separation does indeed occur for all compositions, as evidenced by the differences in the colour contrast in the optical images. This phase separation is more obvious and appears coarser as the amount of Na^+ increased, and is especially evident at 50% Na^+ composition. This observation is also consistent with the possibility of two conduction processes occurring in these ionomers. If these materials are truly random copolymers, then this phase separation is challenging to understand, unless the Mw distribution is bimodal, which could lead to phase separation.[31] Alternatively, these copolymers could be more block-like which has been shown to result in phase separation.[32] The presence of two different cation counterions may also play a role in the observed phase separation, for example if the cations appeared in 'blocks' rather than randomly along the polymer chain.

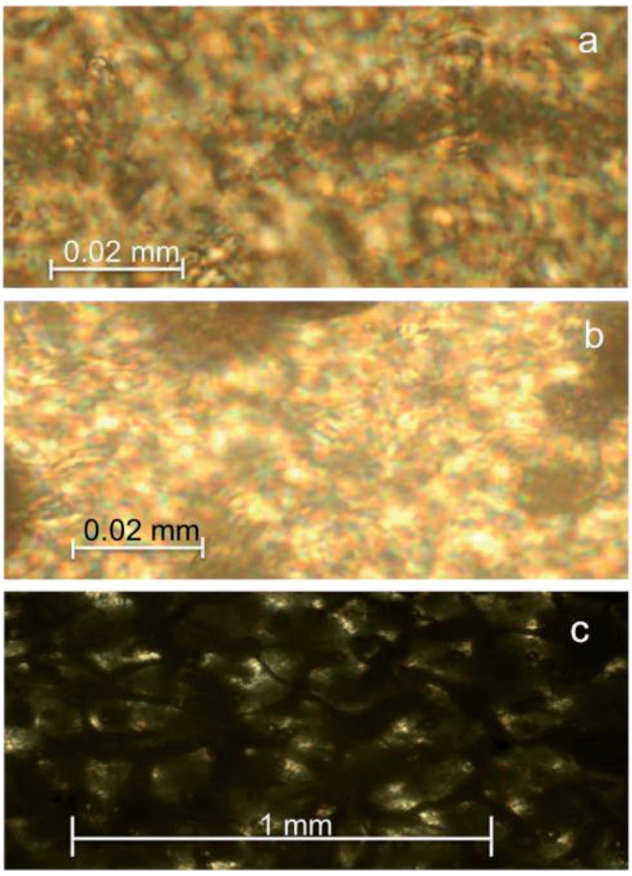

Fig. 6 Optical microscope images of poly([N_{1222}][AMPS]-*co*-Na[VS]) ionomers with various mol% of NaVS (a) 10% (b) 20% (c) 50%.

To understand whether the phase separation is likely due to the presence of large homopolymer blocks within the copolymer or a polymer blend of two different materials we can consider the polymerisation chemistry, however, the reactivity ratios of this combination of monomers are not known. McCormick *et al.*[33,34] reported that polymerisation of sodium AMPS (m1) monomer with [2-(acrylamido)-2-methylpropyl]trimethylammonium chloride (AMPTAC) (m2) formed a water-soluble copolymer with reactivity ratios of $r1 = 0.52$ and $r2 = 0.62$ and this copolymer was strongly alternating. The percentage of homo-blocks was, however, dependent on the monomer feed ratio, while monomer alternation was found to increase with less AMPS monomer in the feed. In addition, the Mw of the homopolymer presented in McCormick's work was lower than the Mw of the copolymer. Other work by Tong *et al.*[35] reported the copolymerisation of AMPS (m1) with 2-hydropropyl methacrylate (HPM) (m2). They discovered that the reactivity ratios for this copolymer are $r1 = 0.04$ and $r2 = 6.30$, and mean sequence length of m1 is shorter than m2. In this case HPM is insoluble in water while AMPS is water soluble. High resolution liquid NMR carried in the present work was unable to distinguish between the various carbons in the copolymer and hence we were not able to characterise the polymer further. However, it appears from the literature discussed above that the reactivity ratios of the monomers are similar and therefore the final ionomer will most likely be a semi-random copolymer of the two monomers.

Solid-state nuclear magnetic resonance (NMR)

Solid-state NMR spectroscopy was used to check the structure and composition of the polymer materials as well as study the dynamic behaviour *via* variable temperature (VT) wideline experiments. The ^{13}C CPMAS spectra (Fig. 7 top) show broad and narrow signals, which can be easily assigned. The narrow signals with chemical shifts of 55.5, 46.7 and 7.2 ppm were assigned to the N–CH_2–, the N–CH_3 and the C–CH_3 groups of the N_{1222} cation, respectively. Line widths between 70 Hz for the methyl signal and 120 Hz for the CH_2 signal are reduced by a factor of 2–3 compared to the matching 220 Hz for the side group methyl signal and 240 Hz and 300 Hz for the side group and backbone CH_2 signals, respectively. This indicates the higher mobility of the ammonium cation in the polymer matrix (mainly rotational but also translational motion). The broad signals are caused by the shorter T_2 of the polymer nuclei due to the inherent lower mobility of the polymer backbone and side groups. Thus the signals from 176, 61, 52.5, 42, 38 to 26 ppm are assigned to the amide carbon, the side group –CH_2–, the

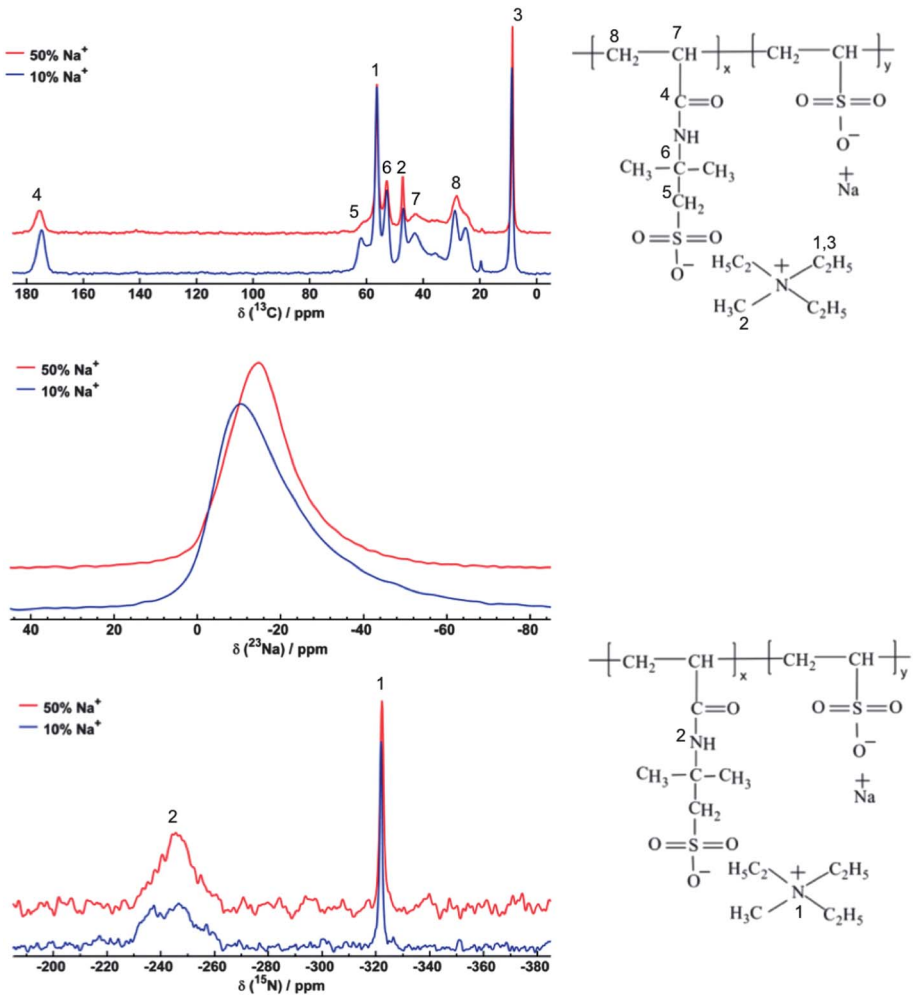

Fig. 7 MAS NMR spectra for ^{13}C, ^{23}Na and ^{15}N (top to bottom) for 10% and 50% Na^+ content.

quaternary carbon, the back bone –CH–, the backbone $–CH_2–$ and the side chain $–CH_3$ group, respectively. The assignment was checked with a CPPI experiment as well as *via* diffusion filtered solution NMR experiments and is in accordance with reported literature shifts of PAMPS polymers.[36]

The ^{23}Na spectra (Fig. 7 middle) both show an asymmetric quadrupolar lineshape which is strongly Gaussian broadened, probably mainly caused by a broad, inhomogeneous distribution of the ^{23}Na chemical environment. It is interesting to note a small shift to lower frequencies for the chemical shift from −5 to −10 ppm with increasing Na^+ content, indicating a small change in the chemical environment (or distribution of environments) of the Na^+ ions. In addition, the ^{15}N CPMAS spectra (Fig. 7 bottom) give two signals that can be assigned to the amide nitrogen (broad due to low mobility and inhomogeneous environment) at −230 to −250 ppm and the quaternary ammonium nitrogen (narrow due to high mobility) at −322 ppm and support the carbon signal assignment. No significant change can be observed in the ^{15}N shifts with increasing Na^+ content.

To study ion dynamics, static wideline ^1H and ^{23}Na spectra at different temperatures were recorded. Assuming a thermally driven motion process is the main cause for nuclear relaxation, a uniform line narrowing of the static NMR signals with increasing temperature would be expected. By measuring static ^{23}Na spectra the $^{23}Na^+$ cation dynamic behaviour is probed. It is important to point out that static ^1H spectra include both components, the signals of the more mobile quaternary ammonium cation and the less mobile polymer, thus the ^1H variable temperature experiments are probing a dynamic behaviour consisting of at least two differing components contributing to the relaxation process.

The ^1H wideline spectra (Fig. 8 top) for the 10% Na^+ containing sample show an inhomogeneous line narrowing, with some narrow components already detectable above 303 K. When approaching T_g (~373 K) an overall line narrowing can be observed, but when keeping the sample slightly below T_g the signals converge into a more homogeneous shape. The differing line widths indicate the presence of inhomogeneous dynamic behaviour in the sample due to partial phase separation. Such inhomogeneity can be removed by annealing the material slightly below T_g. This is consistent with the single impedance arc observed in the conductivity measurement at higher temperatures. The ^{23}Na wideline spectra (Fig. 8 bottom) show

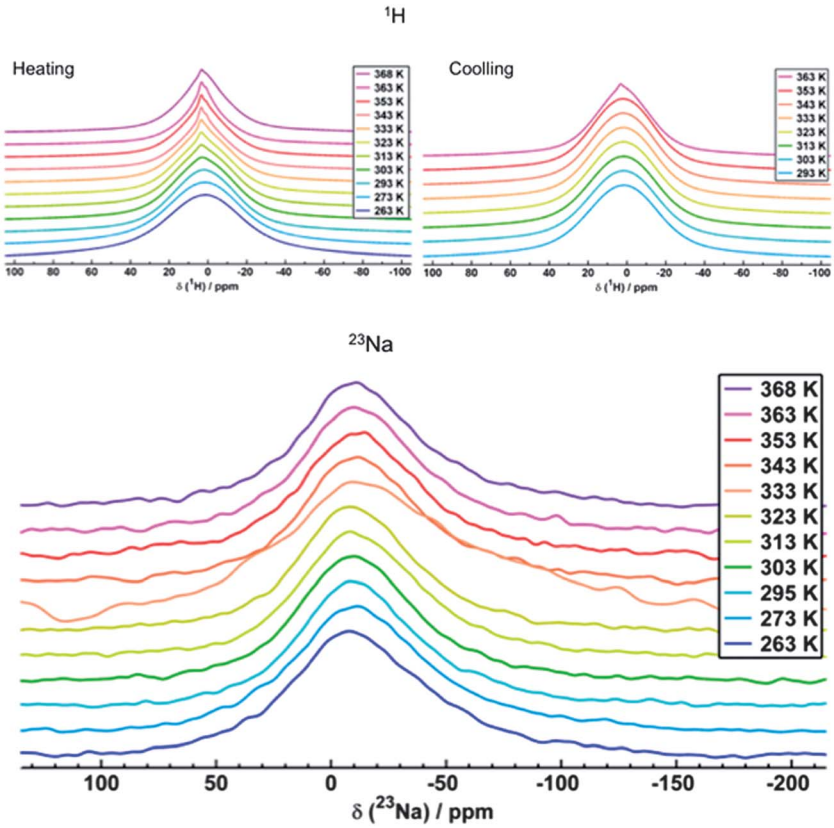

Fig. 8 ^{1}H (top) and ^{23}Na (bottom) VT Wideline NMR spectra of poly([N_{1222}][AMPS]-*co*-Na[VS]) (90 : 10) in the temperature range from 263 to 368 K.

no significant line narrowing but suffer from bad *S*/*N* due to the low Na^+ content. The ^{23}Na lines here are already relatively narrow for a quadrupolar nucleus and thus suggest some degree of mobility is present. The lack of narrowing with increasing temperature may reflect that the linewidth is dominated by an inhomogeneous and distributed environment for the ^{23}Na nucleus, which is highly probable for a quadrupolar nucleus in a changing asymmetric environment.

The effect of 10% PEG additions into the poly([N_{1222}][AMPS]-*co*-Na[VS]) (90 : 10) ionomer

Even though the conductivity measured in these materials appears to be decoupled from the T_g of the ionomer itself, the values are still too low for application in practical devices. Furthermore, we are unable to confirm the role of Na^+ in this conduction process. In order to increase the ionic conductivity and possibly decouple the Na^+ still further from the ionomer backbone, a small amount (10 wt%) of low molecular weight plasticizer, polyethylene glycol (PEG 400) was introduced into the ionomer. Fig. S1† represents the DSC thermogram of poly([N_{1222}][AMPS]-*co*-Na[VS]) (90 : 10) ionomer with 10% PEG. In this sample, a T_g overshoot was not observed in contrast to the sample without PEG. The T_g still appears broad and has decreased by 40 °C to a value of ~50 °C (onset). This indicates that even 10% PEG significantly plasticizes the ionomer, possibly by interacting with the Na^+ ions as we hypothesized, thereby reducing the coulombic interactions between the cation and the polymer backbone.

The conductivity of the PEG plasticized ionomer was also measured upon both heating and cooling cycles. As can be seen from the Nyquist plot Fig. S2,† only one semicircle can be observed in both cycles. This is consistent with only one conduction process in this system, which suggests that the phase separation may no longer be present. The optical microscopy of these plasticized ionomers (as shown in the insert picture in Fig. 9) further confirms that the addition of PEG leads to a more homogeneous material. Significantly, the conductivity was found to increase by four orders of magnitude at room temperature as shown in Fig. 9 and reaches 10^{-5} S cm^{-1} at T_g. Therefore this system also shows strong decoupling of the ionic conductivity from the T_g. This increase in conductivity may arise for either higher mobility of the N_{1222}^{+} cation, or from the additional contribution of the Na^+ ion. ^{23}Na NMR was used to try to provide further insights into the mobility in these systems as discussed below.

The addition of plasticizer had an observable effect on the ^{23}Na static NMR spectra (see Fig. 10a). Compared to the 10% Na^+ sample the half width increased by nearly a factor 2 from 5 kHz to 8.5 kHz for the 10% PEG sample. Whereas the linewidth for both materials only changes slightly with increasing temperature. Fig. 10b shows the effect of temperature on the

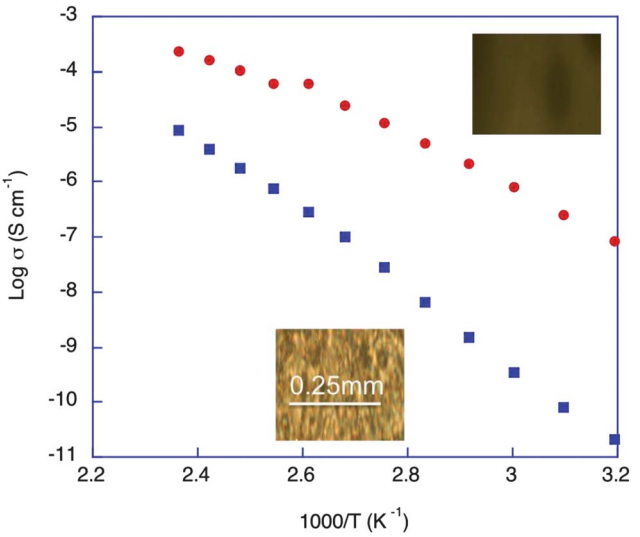

Fig. 9 The ionic conductivity along with the optical images of the poly([N_{1222}][AMPS]-*co*-Na[VS]) (90 : 10) (blue data) with 10% PEG (red data).

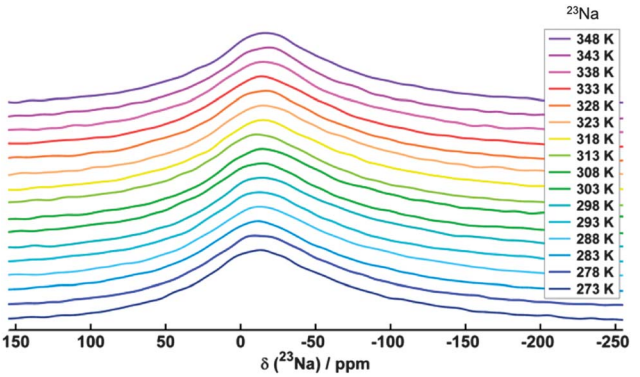

Fig. 10 NMR spectra of ^{23}Na poly ([N_{1222}][AMPS]-*co*-Na[VS]) (90 : 10) with 10% PEG.

^{23}Na chemical shift for the pure and PEG containing ionomer and it is apparent that the addition of PEG changes the overall environment of the Na^+ ion. The more negative chemical shift could reflect a decreasing interaction with the sulfonate anion and a stronger interaction with the PEG oxygens in the plasticized sample. Furthermore, whilst there is a significant degree of scatter in the data, the overall trend does seem to favour a shift to more negative chemical shifts in both systems, which again may reflect less association with the ionomer backbone. The broader lines for the plasticizer added sample show either a higher distribution of frequencies and thus a broader distribution of chemical environments for the sodium ions, or an even lower T_2 value, which could arise from a rapid exchange between very different environments. This provides evidence that the presence of the PEG plasticizer as well as a competing counter ion in the ionomer, means that the sodium ions are less strongly coordinated to the ionomer backbone and are likely distributed (and possibly exchanging) amongst varying environments. The minor change in linewidth and shift relative to varying temperature indicates that the plasticizer does not significantly influence the dynamic behavior of the sodium ions but only the distribution width of sodium coordination. This NMR data correlate well with the observations from DSC and conductivity measurements.

Conclusions

The preparation and characterization of a series of sulfonate based copolymer ionomers with mixtures of ionic liquid and sodium cations have been reported. The T_g, ^{15}N and ^{23}Na chemical shift of ionomers do not vary significantly as the amount of Na^+ changes, while the ionic conductivity increased with decreasing Na^+ composition. The data show that the conductivity is increasingly decoupled from the T_g of the ionomer systems as Na^+ concentration is decreased. The presence of a broad T_g, asymmetric quadrupolar lineshape of ^{23}Na in NMR spectra and two semicircles observed in the impedance diagrams suggests two conduction processes are present in these ionomer systems, and indicates inhomogeneity or phase separation in these materials. The optical microscope images confirm the presence of phase separation in all compositions. An ether based plasticizer, PEG, has been introduced into the ionomer to further improve the ionic conductivity and possibly decouple the Na^+ further from the ionomer backbone. The reduction in T_g and increasing of ionic conductivity shows that even 10% of PEG significantly plasticized the ionomer and increased the conductivity by several orders of magnitude. Furthermore, the impedance and optical microscopy data suggests that the addition of PEG, also leads to a more homogeneous material.

Acknowledgements

The authors are grateful to the Australian Research Council for funding *via* DP130101652 and under the Laureate Fellowship scheme (MF and DRM). We also acknowledge the ARC for support of the NMR facility through the grant LE110100141.

References

1 D. E. Fenton, J. M. Parker and P. V. Wright, *Polymer*, 1973, **14**, 589.
2 S. Lascaud, M. Perrier, M. Armand, J. Prud'homme, B. Kapfer, A. Vallée and M. Gauthier, *Electrochim. Acta*, 1998, **43**, 1407–1414.
3 D. Benrabah, S. Sylla, F. Alloin, J. Y. Sanchez and M. Armand, *Electrochim. Acta*, 1995, **40**, 2259–2264.
4 F. M. Gray, *Solid polymer electrolytes: fundamentals and technological applications*, New York, NY, VCH, New York, NY, 1991.
5 S. H. Chung, Y. Wang, L. Persi, F. Croce, S. G. Greenbaum, B. Scrosati and E. Plichta, *J. Power Sources*, 2001, **97–98**, 644–648.
6 B. Scrosati, F. Croce and S. Panero, *J. Power Sources*, 2001, **100**, 93–100.

7 M. Marcinek, A. Bac, P. Lipka, A. Zalewska, G. Zukowska, R. Borkowska and W. Wieczorek, *J. Phys. Chem. B*, 2000, **104**, 11088–11093.
8 W. Wieczorek, D. Raducha, A. Zalewska and J. R. Stevens, *J. Phys. Chem. B*, 1998, **102**, 8725–8731.
9 S. R. Mohapatra, A. K. Thakur and R. N. P. Choudhary, *Ionics*, 2008, **14**, 255–262.
10 W. Wang, W. Liu, G. J. Tudryn, R. H. Colby and K. I. Winey, *Macromolecules*, 2010, **43**, 4223–4229.
11 C. Tiyapiboonchaiya, J. M. Pringle, D. R. MacFarlane, M. Forsyth and J. Z. Sun, *Macromol. Chem. Phys.*, 2003, **204**, 2147–2154.
12 H. I. Ünal and H. Yilmaz, *J. Appl. Polym. Sci.*, 2002, **86**, 1106–1112.
13 M. Annala, S. Lipponen, T. Kallio and J. Seppälä, *J. Appl. Polym. Sci.*, 2012, **124**, 1511–1519.
14 H. Hu, W. Liu, L. Yang, M. Xiao, S. Wang, D. Han and Y. Meng, *Int. J. Hydrogen Energy*, 2012, **37**, 4553–4562.
15 A. A. Santiago, J. Vargas, J. Cruz-Gómez, M. A. Tlenkopatchev, R. Gaviño, M. López-González and E. Riande, *Polymer*, 2011, **52**, 4208–4220.
16 L. Sun, J. Guo, J. Zhou, Q. Xu, D. Chu and R. Chen, *J. Power Sources*, 2012, **202**, 70–77.
17 G. J. Tudryn, M. V. O'Reilly, S. Dou, D. R. King, K. I. Winey, J. Runt and R. H. Colby, *Macromolecules*, 2012, **45**, 3962–3973.
18 C. Tiyapiboonchaiya, D. R. MacFarlane, J. Sun and M. Forsyth, *Macromol. Chem. Phys.*, 2002, **203**, 1906–1911.
19 N. Byrne, P. C. Howlett, D. R. MacFarlane and M. Forsyth, *Adv. Mater.*, 2005, **17**, 2497–2501.
20 J. Travas-Sejdic, R. Steiner, J. Desilvestro and P. Pickering, *Electrochim. Acta*, 2001, **46**, 1461–1466.
21 M. J. Park and S. Y. Kim, *J. Polym. Sci., Part B: Polym. Phys.*, 2013, **51**, 481–493.
22 P. G. Bekiarian, M. Doyle, W. B. Farnham, A. E. Feiring, P. A. Morken, M. G. Roelofs and W. J. Marshall, *J. Fluorine Chem.*, 2004, **125**, 1187–1204.
23 W. Wang, G. J. Tudryn, R. H. Colby and K. I. Winey, *J. Am. Chem. Soc.*, 2011, **133**, 10826–10831.
24 G. J. Tudryn, W. Liu, S. W. Wang and R. H. Colby, *Macromolecules*, 2011, **44**, 3572–3582.
25 A. S. Best, P. J. Newman, D. R. MacFarlane, K. M. Nairn, S. Wong and M. Forsyth, *Solid State Ionics*, 1999, **126**, 191–196.
26 H. Morimoto, H. Awano, J. Terashima, Y. Shindo, S. Nakanishi, N. Ito, K. Ishikawa and S. I. Tobishima, *J. Power Sources*, 2013, **240**, 636–643.
27 J. L. Sudworth, *J. Power Sources*, 1984, **11**, 143–154.
28 J. Coetzer, *J. Power Sources*, 1986, **18**, 377–380.
29 A. R. Berens and I. M. Hodge, *Macromolecules*, 1982, **15**, 756–761.
30 I. M. Hodge and A. R. Berens, *Macromolecules*, 1982, **15**, 762–770.
31 Z. J. Zhang, Z. Y. Lu and Z. S. Li, *Chin. J. Polym. Sci.*, 2009, **27**, 493–500.
32 L. Leibler, *Macromolecules*, 1980, **13**, 1602–1617.
33 C. L. McCormick and C. B. Johnson, *Macromolecules*, 1988, **21**, 694–699.
34 C. L. McCormick and L. C. Salazar, *Macromolecules*, 1992, **25**, 1896–1900.
35 Z. Tong, Y. Yi and X. Liu, *Polym. Bull.*, 1995, **35**, 591–597.
36 P. Shestakova, R. Willem and E. Vassileva, *Chem.–Eur. J.*, 2011, **17**, 14867–14877.

